ACI STRUCTURAL JOURNAL TECHNICAL PAPER

Title No. 120-S100

Chord Rotation Capacity and Strength of Diagonally Reinforced Concrete Coupling Beams

by A. Lepage, R. D. Lequesne, A. S. Weber-Kamin, S. Ameen, and M.-Y. Cheng

A database of results from 27 tests of diagonally reinforced concrete coupling beams was analyzed to develop improved force-deformation envelopes (backbone curves) for modeling and analysis of coupling beams. The database, which was selected from a larger set of 60 test results, comprises specimens that generally satisfy ACI 318-19 requirements. The analyses show that the chord rotation capacity of diagonally reinforced concrete coupling beams compliant with ACI 318-19 is closely correlated with beam clear span-to-overall depth ratio and, to a lesser extent, the ratio of hoop spacing to diagonal bar diameter. A simple expression is proposed for estimating beam chord rotation capacity. Coupling beam strength was shown to be more accurately estimated from flexural strength calculations at beam ends than other methods. Recommendations are made for obtaining more accurate backbone curves in terms of chord rotation capacity, strength, and stiffness.

Keywords: backbone curve; beam aspect ratio; confining reinforcement; database; deformation capacity; force-deformation envelope; hoop spacing; reinforcement grade; shear stress.

INTRODUCTION

Coupled structural walls are a common lateral force-resisting system in buildings designed for earthquakes. Studies of the behavior of coupling beams subjected to displacement reversals have shown that beams reinforced with diagonally oriented reinforcing bars exhibit large strength and deformation capacity.[1,2] Since ACI 318-99,[3] which first required diagonal reinforcement in short and highly stressed coupling beams, diagonally reinforced coupling beams have become common in practice.

Nonlinear response history analysis of buildings is permitted by ASCE/SEI 7-16[4] as part of the design of any structure. This type of analysis is common in the design and assessment of high-rise buildings with coupled walls. Appendix A in ACI 318-19[5] complements ASCE/SEI 7-16[4] with additional analysis and modeling requirements for the design of new reinforced concrete structures. For evaluation and retrofit of existing buildings, ASCE/SEI 41-17[6] and ACI CODE-369.1-22[7] provide the generalized force-deformation relationship shown in Fig. 1. ASCE/SEI 41-17[6] defines the envelope in Fig. 1 using the parameters in Table 1, which are also permitted by Appendix A in ACI 318-19.[5] The data in Fig. 1 and Table 1 will be referred to as the ASCE/SEI 41-17[6] envelope.

Figure 1 and Table 1 suggest that well-detailed diagonally reinforced coupling beams exhibit their peak strength at or beyond a chord rotation of 0.03 rad and retain 80% of their strength Q_y to a chord rotation of at least 0.05 rad. These deformation parameters underestimate the chord rotation capacity of well-detailed slender coupling beams ($\ell_n/h >$ 3). Naish et al.[2,9] reported that coupling beams with ℓ_n/h = 3.3 exhibit peak strengths at chord rotations exceeding 0.05 rad and can retain strengths of $0.8V_m$ to chord rotations exceeding 0.08 rad. Recent test results[10,11] furthermore suggest that chord rotation capacity is related to ℓ_n/h, with beams retaining residual strengths of $0.8V_m$ to 0.05 rad when ℓ_n/h = 1.5 and approaching 0.07 rad for ℓ_n/h = 3.5. Test data therefore suggest that deformation capacity parameters in Table 1 should account for ℓ_n/h. Effects of other parameters including bar grade, concrete strength, shear stress, transverse reinforcement detailing, axial restraint, and other variables should be investigated.

Parameters in Table 1 for coupling beam strength are a function of Eq. (1), which is based on the ACI 318-19[5] provisions for diagonally reinforced coupling beams. This equation attributes the entire beam strength to the diagonal reinforcement, neglecting the shear strength attributable to hoops and the flexural strength resulting from any non-diagonal reinforcement developed into the walls. The ASCE/SEI 41-17[6] envelope uses Eq. (1) (with expected material properties instead of specified values) to define the strength Q_y at point B. The peak strength Q_C is $1.25Q_y$, and the residual strength is $0.8Q_y$. Studies have shown this approach can substantially underestimate beam strength,[10-14] with reported measured strengths that were 30 to 100% larger than Q_y when all non-diagonal bars terminated near the beam end (and 40 to over 200% more than Q_y when non-diagonal bars extended into the supports). It is not necessarily conservative to underestimate expected beam strength because beam shear strengths contribute to force demands in wall piers and foundations.[15,16] Research shows that the shear corresponding to the beam developing its nominal flexural strength at both ends $(M_n^+ + M_n^-)/\ell_n$ provides a considerably more accurate estimate of beam strength than Eq. (1).[10-14] Determining beam shear based on M_n also allows accounting for the effects of slabs and axial restraint.

$$\begin{aligned} V_{n,\text{Eq.(1)}} &= 2A_{vd}f_y\sin\alpha \le 10\sqrt{f_c'}b_w h \quad \text{(in.-lb)} \\ V_{n,\text{Eq.(1)}} &= 2A_{vd}f_y\sin\alpha \le 0.83\sqrt{f_c'}b_w h \quad \text{(metric)} \end{aligned} \tag{1}$$

ACI Structural Journal, V. 120, No. 6, November 2023.
MS No. S-2022-337.R1, doi: 10.14359/51739092, received May 15, 2023, and reviewed under Institute publication policies.

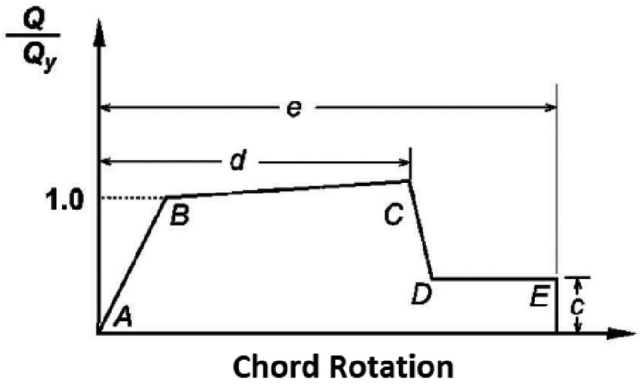

Fig. 1—Generalized force-deformation relationship defined in ASCE/SEI 41-17 Fig. 10-1(b),[6] similar to ACI CODE-369.1-22 Fig. 3.1.2.2.3(b).[7]

Table 1 shows that the ASCE/SEI 41-17[6] envelope defines coupling beam stiffness based on an effective moment of inertia of $0.3I_g$, even though coupling beam specimens often exhibit stiffnesses closer to $0.15I_g$.[9] TBI[8] recommends Eq. (2), which closely approximates the effective stiffness of coupling beams reinforced with Grade 60 (420) bars. When multiplied by $60/f_y$, ksi ($420/f_y$, MPa), the resulting equation (Eq. (3)) works well for coupling beams with Grade 60 to 120 (420 to 830) bars.[17]

$$I_{eff}/I_g = 0.07(\ell_n/h) \quad (2)$$

$$I_{eff}/I_g = 0.07(\ell_n/h)(60/f_y) \text{ (in.-lb)}$$
$$I_{eff}/I_g = 0.07(\ell_n/h)(420/f_y) \text{ (metric)} \quad (3)$$

Although the simplicity of the parameters in Table 1 is desirable, improvements to the parameters for chord rotation capacity, strength, and stiffness are possible. This paper reports analyses of a database of diagonally reinforced coupling beam specimens tested under reversed cyclic loads. The two main motivations were to: 1) identify the variables that most affect coupling beam deformation capacity and propose a simple equation that represents the deformation capacity of coupling beam specimens; and 2) assess the accuracy of Eq. (1) and alternative methods for calculating the expected strength of diagonally reinforced concrete coupling beams.

RESEARCH SIGNIFICANCE

This paper reports analyses of a database of results from tests of diagonally reinforced coupling beams. The analyses support revising the force-deformation envelope (backbone curves) recommended in ASCE/SEI 41-17[6] and ACI CODE-369.1-22[7] for modeling and analysis of coupling beams. Specific recommendations are made, and the resulting backbone curves are compared against sample test results. These recommendations aim to improve the state of engineering practice in the analysis and design of buildings with structural walls and coupling beams.

COUPLING BEAM DATABASE

A database of results from tests of 60 diagonally reinforced coupling beams was assembled.[18] From this database, a smaller "analysis" database was selected,[19] comprising 27 specimens. Refer to Table 2 for the data summary and the Notation section for definitions. The following describes how specimens were selected from the literature and the criteria used to select specimens for the analysis database. The contents of the analysis database are briefly reported; more details, including reasons for excluding individual specimens from the analysis database, are available in References 11 and 19.

Table 1—Force-deformation envelope for nonlinear procedures

Parameters*		Envelope from ASCE/SEI 41-17[6]
Deformation capacity	d	0.03
	e	0.05
Strength	Q_y	$V_{n,\text{Eq.(1)}}$†
	Q_C	V_{pr}‡
	c	0.8
Stiffness	I_{eff}/I_g	0.3§

*Refer to Notation.

†Equation (1) using expected yield stress, $f_{y,e}$.

‡Equation (1) using $1.25f_{y,e}$.

§Based on Table 10-5 of ASCE/SEI 41-17. Reference 8 recommends 0.07 (ℓ_n/h) instead of 0.3.

Database description

The 60 specimens in the full database[18] satisfy the following criteria: 1) enough information was available describing the specimens to support the analyses described herein; 2) the beam was reinforced with straight (not bent) diagonal bars throughout the beam clear span that were continuously bonded to the concrete; 3) the beam contained no fiber reinforcement or structural steel sections; 4) the concrete was confined with rectilinear hoops enclosing either the diagonal bar groups or the full beam section; 5) the beam was subjected to reversed cyclic displacements and double curvature; 6) the failure mode did not include twisting due to inadequate out-of-plane bracing; and 7) the beam was prismatic and without penetrations or notches.

Table 2 contains the subset of 27 specimens selected to form an analysis database.[19] In addition to the conditions listed previously, the specimens in Table 2 also meet the following criteria: 1) diagonal bar confinement spacing was nominally consistent throughout the span; 2) the ratio of transverse reinforcement spacing to diagonal bar diameter (s/d_b) was less than or equal to 6; 3) the average of the maximum axial forces imposed in each loading direction was measured, reported, and not larger than $0.15A_gf_{cm}$; 4) a systematic loading protocol consisting of fully reversed cyclic displacements with increasing amplitude was used, and testing was continued until beam strength diminished to less than 80% of the peak strength; 5) beams had a rectangular cross section (that is, not integral with a slab); and 6) the least cross-sectional dimension was not less than 5 in. (125 mm). These limits were imposed so specimens in the analysis database would generally represent beams conforming to requirements of ACI 318-19.[5] The

Table 2—Database of diagonally reinforced coupling beams included in derivation of equation for chord rotation capacity

Specimen number			1	2	3	4	5	6	7	8	9	10	11	12	13
Reference			Naish et al.[2]			Lim et al.[20]		Lim et al.[21]		Cheng et al.[10]					
Specimen ID			CB24D	CB24F	CB33F	CB30-DA	CB30-DB	CB10-1	CB20-1	D1.5_H	D1.5_H2	D1.5_L	D2.5_H	D2.5_L	D3.5_L
Beam properties	b_w	in.	12.0	12.0	12.0	11.8	11.8	9.84	11.8	11.0	11.0	11.0	11.0	11.0	11.0
	h	in.	15.0	15.0	18.0	19.7	19.7	19.7	19.7	19.0	19.0	19.0	19.0	19.0	19.0
	Confinement*		Diag.	Full	Full	Diag.	Full	Full	Full	Full	Full	Full	Full	Full	Full
	$b_c \perp b_w$	in.	8.125	9.50	9.50	5.98	10.2	8.27	10.2	9.00	9.00	9.00	9.00	9.00	9.00
	$b_c \perp h$	in.	4.00	13.5	16.5	5.20	16.5	16.5	16.5	17.0	17.0	17.0	17.0	17.0	17.0
	ℓ_n	in.	36.0	36.0	60.0	59.1	59.1	19.7	39.4	28.0	28.0	28.0	47.0	47.0	67.0
	ℓ_n/h		2.40	2.40	3.33	3.00	3.00	1.00	2.00	1.47	1.47	1.47	2.47	2.47	3.53
	f_{cm}	psi	6850	6850	6850	5750	5550	5000	7550	6600	7000	4400	5100	4700	6800
Diagonal reinforcement	Quantity	ea. diag.	6	6	6	4	4	4	4	8	4	4	6	4	4
	α	degrees	15.7	15.7	12.3	8.80	8.80	26.0	16.0	20.9	18.5	20.9	12.5	9.00	8.90
	d_b	in.	0.875	0.875	0.875	1.27	1.27	1.00	1.13	0.750	1.13	0.750	1.13	1.13	1.13
	f_{ym}	ksi	70.0	70.0	70.0	67.4	67.4	70.4	67.6	66.2	66.8	69.5	70.8	70.8	66.8
Parallel reinforcement	Quantity	total	10	10	12	4	10	10	10	6	6	6	6	6	6
	d_{bp}	in.	0.250	0.375	0.375	0.500	0.375	0.375	0.500	0.500	0.500	0.500	0.500	0.500	0.500
	f_{ym}	ksi	70.0	70.0	70.0	64.0	68.9	68.9	72.8	61.9	61.9	64.1	64.1	64.1	61.9
	Condition†		Cut	Cut	Cut	Devel.	Devel.	Devel.	Devel.	Cut	Cut	Cut	Cut	Cut	Cut
Transverse reinforcement	d_{bt}	in.	0.375	0.375	0.375	0.375	0.375	0.500	0.500	0.500	0.500	0.500	0.500	0.500	0.500
	f_{ytm}	ksi	70.0	70.0	70.0	68.9	68.9	67.9	72.8	120	120	125	125	125	120
	s	in.	2.50	3.00	3.00	5.91	3.94	3.94	3.94	4.33	4.33	4.33	4.50	4.50	4.33
	s/d_b		2.86	3.43	3.43	4.65	3.10	3.94	3.49	5.78	3.84	5.78	3.99	3.99	3.84
	$(s/d_b)\sqrt{f_{ym}/60\text{ ksi}}$		3.09	3.70	3.70	4.93	3.29	4.27	3.71	6.07	4.05	6.22	4.33	4.33	4.05
	$\frac{A_{sh,provided}}{sb_c} \perp b_w$‡, %		1.62	1.16	1.16	0.62	0.82	1.01	0.82	1.03	1.03	1.03	0.99	0.99	1.03
	$\frac{A_{sh,provided}}{sb_c} \perp h$‡, %		2.20	1.09	1.11	0.72	0.68	0.68	0.68	0.81	0.81	0.81	0.78	0.78	0.81
	$\frac{A_{sh,provided}}{A_{sh,required}} \perp b_w$‡		1.84	1.31	1.31	0.83	1.13	1.53	0.88	2.07	1.95	3.24	2.69	2.92	2.01
	$\frac{A_{sh,provided}}{A_{sh,required}} \perp h$‡		2.50	1.23	1.26	0.95	0.93	1.02	0.72	1.65	1.55	2.57	2.14	2.32	1.60
V_m	–	kip	155	171	109	154	156	315	241	347	378	209	237	173	166
	+	kip	159	150	124	151	164	325	234	356	401	221	238	178	163
v_{max}	$\frac{v_{max}}{b_w h\sqrt{f_{cm}, \text{psi}}}$		10.7	11.5	6.9	8.7	9.5	23.7	11.9	21.0	22.9	15.9	15.9	12.4	9.6
$CR_{cap,m}$	–	%	8.50	9.00	8.00	7.40	8.40	5.80	7.70	5.40	5.10	4.70	5.90	6.70	6.30
	+	%	8.80	10.0	8.10	7.00	7.50	6.20	8.20	5.70	5.40	5.30	6.90	6.00	7.10
	Avg.	%	8.65	9.50	8.05	7.20	7.95	6.00	7.95	5.55	5.25	5.00	6.40	6.35	6.70
Axial restraint			No	No	No	No	No	No	No	Yes	Yes	Yes	Yes	Yes	Yes

*Diag. is confinement of each diagonal bar group; Full is confinement of entire beam cross section (except concrete cover).

†Cut is secondary longitudinal bars cut off near support face; Devel. is secondary longitudinal bars developed into supports.

‡$\perp b_w$ is transverse reinforcement perpendicular to beam width; $\perp h$ is transverse reinforcement perpendicular to beam depth.

Note: 1 in. = 25.4 mm; 1 ksi = 1000 psi = 6.89 MPa; 1 kip = 4.45 kN.

small number of specimens with slabs were omitted from the analysis database to remove a variable that could not be easily evaluated due to the limited data. The specimens with axial forces larger than $0.15A_g f_{cm}$, or with axial restraint and an unknown magnitude axial force, were also excluded due to the limited data available. The effects of slabs and axial forces on chord rotation capacity are addressed later.

Table 2, cont.—Database of diagonally reinforced coupling beams included in derivation of equation for chord rotation capacity

Specimen number			14	15	16	17	18	19	20	21	22	23	24	25	26	27
Reference			Ameen et al.[17]					Weber-Kamin et al.[11]								
Specimen ID			CB1	CB2	CB2AD	CB2D	CB3D	D80-1.5	D80-2.5	D80-3.5	D100-1.5	D100-2.5	D100-3.5	D120-1.5	D120-2.5	D120-3.5
Beam properties	b_w	in.	10.0	10.0	10.0	10.0	10.0	12.0	12.0	12.0	12.0	12.0	12.0	12.0	12.0	12.0
	h	in.	18.0	18.0	18.0	18.0	18.0	18.0	18.0	18.0	18.0	18.0	18.0	18.0	18.0	18.0
	Confinement*		Full	Full	Full	Full	Full	Full	Full	Full	Full	Full	Full	Full	Full	Full
	$b_c \perp b_w$	in.	8.50	8.50	8.50	8.50	8.50	10.5	10.5	10.5	10.5	10.5	10.5	10.5	10.5	10.5
	$b_c \perp h$	in.	16.5	16.5	16.5	16.5	16.5	16.5	16.5	16.5	16.5	16.5	16.5	16.5	16.5	16.5
	ℓ_n	in.	34.0	34.0	34.0	34.0	34.0	27.0	45.0	63.0	27.0	45.0	63.0	27.0	45.0	63.0
	ℓ_n/h		1.89	1.89	1.89	1.89	1.89	1.50	2.50	3.50	1.50	2.50	3.50	1.50	2.50	3.50
	f_{cm}	psi	6000	7200	5650	6300	6200	7600	8400	7800	8200	8000	7900	7600	7800	8200
Diagonal reinforcement	Quantity	ea. diag.	6	4	4	4	6	6	9	9	5	7	9	4	6	8
	α	degrees	18.0	18.0	18.0	18.0	18.0	22.7	14.2	10.0	22.7	14.2	10.3	22.7	14.2	10.3
	d_b	in.	0.875	0.750	0.750	0.750	0.750	0.750	0.750	0.875	0.750	0.750	0.750	0.750	0.750	0.750
	f_{ym}	ksi	63.0	128	128	128	128	83.0	83.0	84.0	108	108	108	116	116	116
Parallel reinforcement	Quantity	total	8	8	8	8	8	10	10	10	10	10	10	10	10	10
	d_{bp}	in.	0.375	0.375	0.375	0.375	0.375	0.375	0.375	0.375	0.375	0.375	0.375	0.375	0.375	0.375
	f_{ym}	ksi	69	69	69	69	69	89.0	89.0	89.0	89.0	89.0	89.0	89.0	133	89.0
	Condition†		Cut	Cut	Devel.	Devel.	Devel.	Cut	Cut	Cut	Cut	Cut	Cut	Cut	Devel.	Cut
Transverse reinforcement	d_{bt}	in.	0.375	0.375	0.375	0.375	0.375	0.375	0.375	0.375	0.375	0.375	0.375	0.375	0.375	0.375
	f_{ytm}	ksi	68.0	68.0	68.0	68.0	68.0	89.0	89.0	89.0	89.0	89.0	89.0	89.0	133	89.0
	s	in.	3.00	3.00	3.00	3.00	3.00	3.00	3.00	3.00	3.00	3.00	3.00	3.00	3.00	3.00
	s/d_b		3.43	4.00	4.00	4.00	4.00	4.00	4.00	3.43	4.00	4.00	4.00	4.00	4.00	4.00
	$(s/d_b)\sqrt{f_{ym}/60\text{ ksi}}$		3.51	5.84	5.84	5.84	5.84	4.70	4.70	4.06	5.37	5.37	5.37	5.56	5.56	5.56
	$\frac{A_{sh,provided}}{sb_c} \perp b_w$‡, %		0.86	0.86	0.86	0.86	0.86	1.05	1.05	1.05	1.05	1.05	1.05	1.05	1.05	1.05
	$\frac{A_{sh,provided}}{sb_c} \perp h$‡, %		0.89	0.89	0.89	0.89	0.89	0.89	0.89	0.89	0.89	0.89	0.89	0.89	0.89	0.89
	$\frac{A_{sh,provided}}{A_{sh,required}} \perp b_w$‡		1.09	0.91	1.15	1.03	1.05	1.36	1.23	1.33	1.26	1.29	1.31	1.36	1.98	1.26
	$\frac{A_{sh,provided}}{A_{sh,required}} \perp h$‡		1.12	0.93	1.19	1.07	1.08	1.16	1.05	1.13	1.07	1.10	1.11	1.16	1.68	1.07
V_m	–	kip	184	192	234	194	268	239	220	218	257	220	192	262	283	216
	+	kip	182	207	228	204	275	254	218	219	252	214	196	264	286	212
v_{max}	$\frac{v_{max}}{b_w h\sqrt{f_{cm},\text{psi}}}$		13.2	13.6	17.3	14.3	19.4	13.5	11.1	11.5	13.1	11.4	10.2	14.0	15.0	11.0
$CR_{cap,m}$	–	%	7.00	4.60	5.50	5.40	5.20	6.40	6.90	8.40	4.70	5.30	6.90	5.40	6.70	6.60
	+	%	8.00	5.60	5.30	5.40	6.50	7.30	8.30	8.80	5.80	6.60	6.70	5.00	7.00	6.80
	Avg.	%	7.50	5.10	5.40	5.40	5.85	6.85	7.60	8.60	5.25	5.95	6.80	5.20	6.85	6.70
Axial restraint			No	No	Yes	No	No	No	No	No	No	No	No	No	No	No

*Diag. is confinement of each diagonal bar group; Full is confinement of entire beam cross section (except concrete cover).

†Cut is secondary longitudinal bars cut off near support face; Devel. is secondary longitudinal bars developed into supports.

‡$\perp b_w$ is transverse reinforcement perpendicular to beam width; $\perp h$ is transverse reinforcement perpendicular to beam depth.

Note: 1 in. = 25.4 mm; 1 ksi = 1000 psi = 6.89 MPa; 1 kip = 4.45 kN.

Table 2 reports the main variables (refer to Notation) that define geometry, material properties, reinforcement details, measured strength, and chord rotation capacity for the specimens in the analysis database. Table 3 and Fig. 2 show the range, mean, and distribution of several important variables within the database. The variables include beam width, b_w; beam overall depth, h; aspect ratio, ℓ_n/h; measured concrete compressive strength, f_{cm}; measured yield stress of the

Table 3—Range of values for main variables in analysis database for diagonally reinforced coupling beams

	b_w, in. (mm)	h, in. (mm)	ℓ_n/h	f_{cm}, psi (MPa)	f_{ym}, ksi (MPa)	s/d_b	$\frac{s}{d_b}\sqrt{\frac{f_{ym}}{60\text{ ksi}}}$	$\frac{v_{max}}{\sqrt{f_{cm}\text{ psi}}}$* (MPa)	$CR_{cap,m}$, %
Min.	9.8 (250)	15 (381)	1.0	4400 (30.3)	63.0 (434)	2.9	3.1	6.9 (0.58)	5.0
Mean	11.3 (287)	18.2 (464)	2.3	6740 (46.4)	88.6 (611)	4.0	4.8	13.7 (1.14)	6.7
Max.	12 (305)	19.7 (500)	3.5	8400 (57.9)	128 (883)	5.8	6.2	23.7 (1.97)	9.5

*Ratios of $2A_{vd}f_{ym}\sin\alpha$ to $\sqrt{f_{cm}\text{ (psi)}}b_w d$ ranged between 4.8 and 14.8 with a mean of 8.8.

Note: 1 ksi = 6.89 MPa.

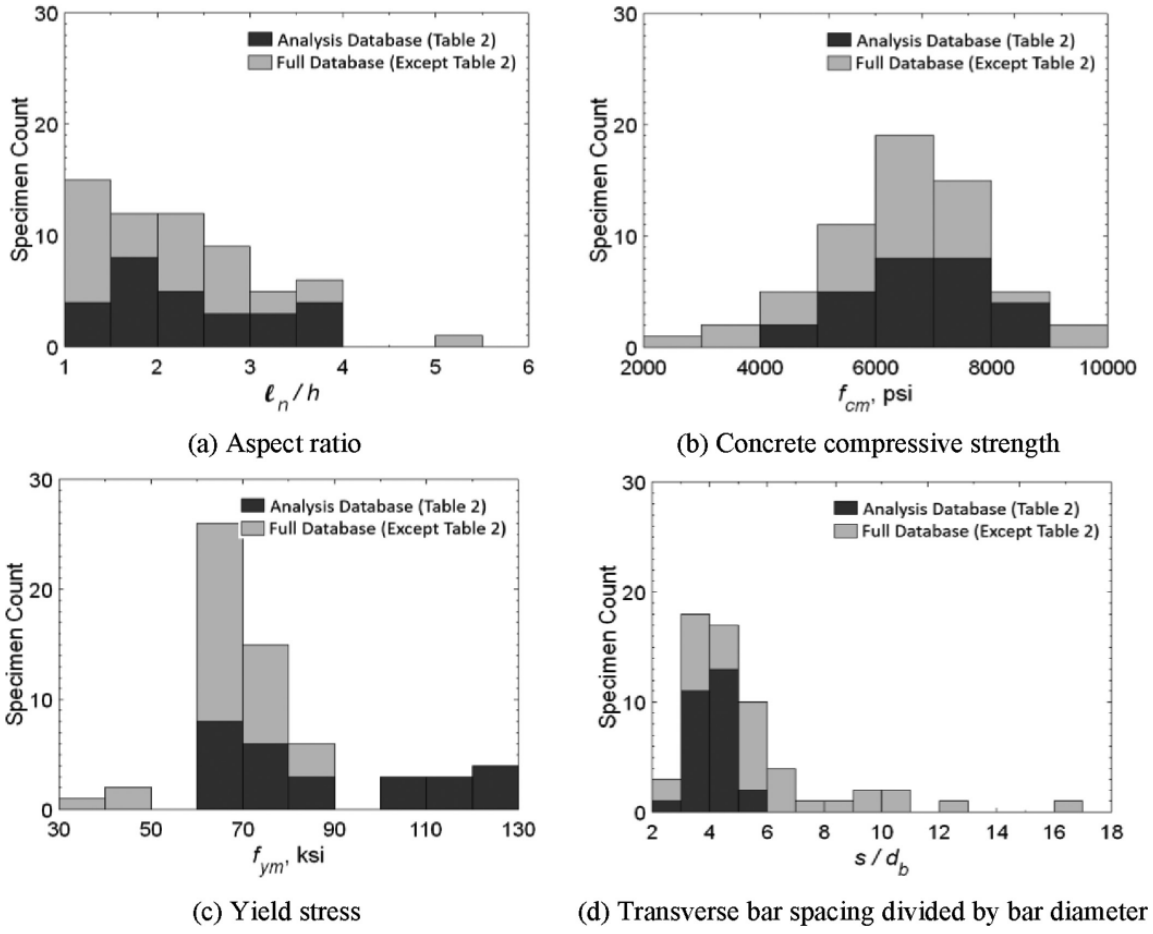

Fig. 2—Histograms of variables within database. (Note: 1 ksi = 1000 psi = 6.89 MPa.)

diagonal reinforcement, f_{ym}; hoop spacing-to-bar diameter ratio, s/d_b; normalized hoop spacing-to-bar diameter ratio, $\overline{s/d_b} = (s/d_b)(\sqrt{f_{ym}/60\text{ ksi}})$ $[(s/d_b)(\sqrt{f_{ym}/420\text{ MPa}})]$; normalized shear stress, $v_{max}/\sqrt{f_{cm}}$; and chord rotation capacity, $CR_{cap,m}$. (Note that s/d_b was normalized by the square root of $f_{ym}/60$ ksi [$f_{ym}/420$ MPa] because the Euler buckling equation indicates buckling stress is inversely proportional to the square of the slenderness ratio, assumed proportional to s/d_b, where d_b and f_{ym} refer to the diagonal bar and s refers to the hoop spacing. This was done for simplicity, although it is acknowledged that the Euler equation represents elastic buckling, while buckling of a diagonal bar is an inelastic phenomenon.) The range and distribution of values shown in Table 3 and Fig. 2 generally show that the analysis database represents ACI 318-19[5]-compliant coupling beams, except specimens with higher strength reinforcement and higher shear stresses are also included.

COUPLING BEAM CHORD ROTATION CAPACITY

Correlations between chord rotation capacity and design variables

Chord rotation capacity was defined for each specimen as the average of the chord rotations in each loading direction where the envelope of the post-peak shear versus chord rotation data (formed by connecting the maximum chord rotation of the first cycle of each loading step) intersected a line at 80% of the maximum applied shear in each loading direction. This definition of chord rotation capacity, which is based on an envelope drawn according to ASCE/SEI 41-17,[6] is less sensitive to the drift increment of the loading protocol than some other definitions because the shear-chord rotation

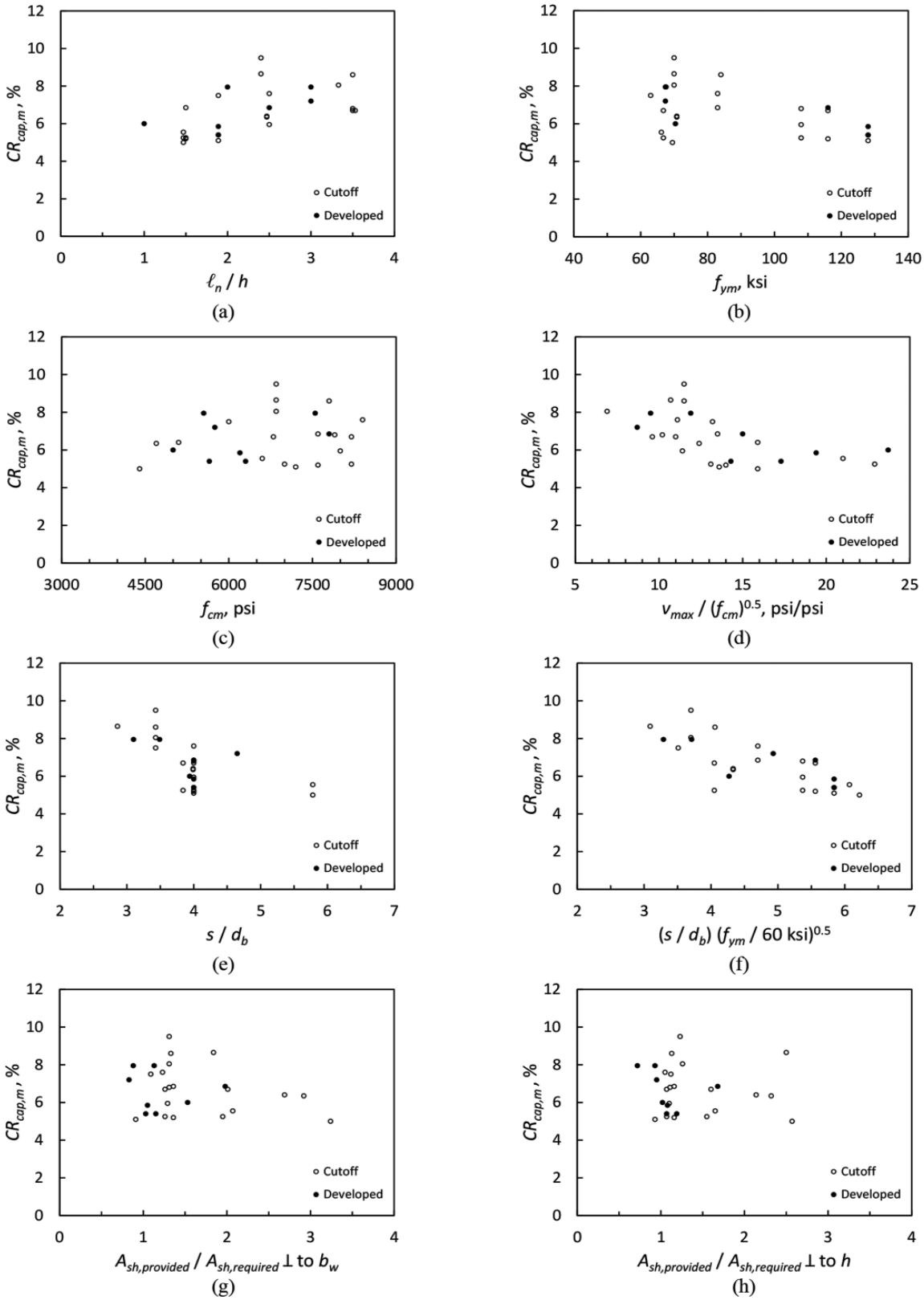

Fig. 3—Chord rotation capacity versus design variables. (Note: 1 ksi = 1000 psi = 6.895 MPa.)

relationship is represented by linear interpolations between measured values.

In Fig. 3, the measured chord rotation capacity ($CR_{cap,m}$) for specimens in the analysis database (Table 2) is plotted against ℓ_n/h, f_{ym}, f_{cm}, $v_{max}/\sqrt{f_{cm}}$, s/d_b, $\overline{s/d_b}$, and $A_{sh,provided}/A_{sh,required}$ (both perpendicular to b_w and h). Beams with cutoff longitudinal bars (not developed into the supports) and beams with developed longitudinal bars are identified with open and solid circles, respectively. Qualitatively, it can be observed that $CR_{cap,m}$ is positively correlated with ℓ_n/h and negatively correlated with s/d_b and $\overline{s/d_b}$. It also appears that $CR_{cap,m}$ is negatively correlated with f_{ym}, but further

Table 4—Summary data for single-variable linear regression of chord rotation capacity versus selected parameters based on Eq. (4)

	ℓ_n/h	f_{ym}	f_{cm}	$\frac{v_{max}}{\sqrt{f_{cm}}\ \text{psi}}$	s/d_b	$\frac{s}{d_b}\sqrt{\frac{f_{ym}}{60\ \text{ksi}}}$	$\frac{A_{sh,provided}^*}{A_{sh,required}}$	
							⊥ to b_w	⊥ to h
c_0†	4.53	8.79	5.39	9.02	11.37	11.37	7.35	6.92
c_1†	0.92	–0.024	0.19/1000	–0.17	–1.19	–0.99	–0.46	–0.20
r^2	0.31	0.22	0.03	0.34	0.37	0.57	0.05	0.01

*⊥ to b_w is transverse reinforcement perpendicular to beam width; ⊥ to h is transverse reinforcement perpendicular to beam depth.

†c_0 and c_1 are constants in Eq. (4), where chord rotation is in percentage units.

Note: 1 ksi = 6.89 MPa.

investigation is needed because the 10 specimens with f_{ym} > 100 ksi (690 MPa) all had $\overline{s/d_b} > 5$, so the apparent correlations with f_{ym} and $\overline{s/d_b}$ are not independent. Likewise, the apparent negative correlation between $CR_{cap,m}$ and $v_{max}/\sqrt{f_{cm}}$ requires further investigation because the apparent correlations with ℓ_n/h and $v_{max}/\sqrt{f_{cm}}$ are not independent (12 of the 14 beams with $v_{max}/\sqrt{f_{cm}} > 13$ psi [1.08 MPa] also had $\ell_n/h < 2$). These interdependencies are addressed later.

Chord rotation capacity does not appear sensitive to $A_{sh,provided}/A_{sh,required}$. Providing $A_{sh,provided}/A_{sh,required} \geq 1$ is important, but Fig. 3 suggests that $CR_{cap,m}$ is not sensitive to $A_{sh,provided}$ in diagonally reinforced beams that satisfy ACI 318-19[5] confinement requirements. This observation should be considered with some caution, as evidence from strain gauges on hoops have shown that transverse reinforcement yielding can be expected under some conditions. For example, coupling beams with developed longitudinal (non-diagonal) bars tend to exhibit less concentrated rotations at the beam ends but more shear distress within the span, which causes larger hoop strain demands.[13,17] It may be advantageous to provide additional transverse reinforcement when all longitudinal bars are developed.

In general, Fig. 3 shows no clear difference between the trends for beams with cutoff longitudinal reinforcement and beams with developed longitudinal reinforcement. This suggests that this detail has little effect on the deformation capacity of well-detailed diagonally reinforced coupling beams, consistent with prior findings.[17]

Using data from Table 2, a simple linear regression was done to quantify the strength of the correlations between $CR_{cap,m}$ and parameters X_i, which were taken as ℓ_n/h, f_{ym}, f_{cm}, $v_{max}/\sqrt{f_{cm}}$, s/d_b, $\overline{s/d_b}$, and $A_{sh,provided}/A_{sh,required}$. An equation with the form of Eq. (4) was fit to each of the eight plots in Fig. 3.

$$CR_{cap,\text{Eq.(4)}} = c_0 + c_1 X_i \tag{4}$$

Table 4 shows the coefficients c_0 and c_1, as well as the coefficient of determination r^2, for each of the resulting eight equations. The coefficients c_0 and c_1 informed initial values for later multivariate regression analyses. Larger values of r^2 suggest stronger correlations between the selected variables and $CR_{cap,m}$.

Table 4 shows that $CR_{cap,m}$ was most strongly correlated with $\overline{s/d_b}$, having $r^2 = 0.57$. The correlations between $CR_{cap,m}$ and ℓ_n/h, $v_{max}/\sqrt{f_{cm}}$, and s/d_b were similar in terms of r^2, with values of 0.31, 0.34, and 0.37, respectively. Table 4 shows that $CR_{cap,m}$ was more weakly correlated with f_{ym}, having $r^2 = 0.22$, and not correlated with f_{cm} and $A_{sh,provided}/A_{sh,required}$, with $r^2 \leq 0.05$.

It was observed previously that f_{ym} and $\overline{s/d_b}$ are not independent within the analysis database because the 10 specimens with f_{ym} > 100 ksi (690 MPa) all had $\overline{s/d_b} > 5$. A trend line for f_{ym} versus $\overline{s/d_b}$ has $r^2 = 0.50$, indicating a relatively strong correlation between these variables within the database. To separate these variables, specimens with f_{ym} > 100 ksi (690 MPa) were removed to produce a subset of 17 specimens with f_{ym} between 63 and 84 ksi (434 and 579 MPa) that have no correlation between f_{ym} and $\overline{s/d_b}$ ($r^2 = 0.01$). When compared against this smaller data set, $CR_{cap,m}$ and $\overline{s/d_b}$ are still relatively strongly correlated ($r^2 = 0.47$), whereas $CR_{cap,m}$ and f_{ym} are not ($r^2 = 0.05$). On this basis, it will be assumed for subsequent analyses that $CR_{cap,m}$ is more strongly dependent on $\overline{s/d_b}$ than f_{ym}.

It was also previously observed that ℓ_n/h and $v_{max}/\sqrt{f_{cm}}$ are not independent within the analysis database because 12 of the 14 beams with $v_{max}/\sqrt{f_{cm}} > 13$ psi (1.08 MPa) also had $\ell_n/h < 2$. A trend line for ℓ_n/h versus $v_{max}/\sqrt{f_{cm}}$ has $r^2 = 0.55$, indicating a relatively strong correlation between these variables within the database. It is therefore not clear from the data in Table 4 whether $CR_{cap,m}$ is correlated with ℓ_n/h, $v_{max}/\sqrt{f_{cm}}$, or both. Studies[10,17] have shown that well-detailed diagonally reinforced coupling beams with the same aspect ratio and different shear stress demands exhibit similar chord rotation capacities. On this basis, the following analyses include ℓ_n/h and not $v_{max}/\sqrt{f_{cm}}$.

Equation for chord rotation capacity

Multiple regression analysis was done using the analysis database (Table 2) to develop an equation for chord rotation capacity (Eq. (5)). Based on the r^2 values in Table 4 and the preceding discussion, ℓ_n/h and $\overline{s/d_b}$ were selected as the primary variables. Both f_{ym} and $v_{max}/\sqrt{f_{cm}}$ were omitted from Eq. (5) for reasons described previously. Although s/d_b was also somewhat correlated with $CR_{cap,m}$, it is omitted from Eq. (5) to avoid redundancy with $\overline{s/d_b}$.

$$CR_{cap,\text{Eq.(5)}} = (9.3 + 0.62\ell_n/h - 0.85\overline{s/d_b})/100 \tag{5}$$

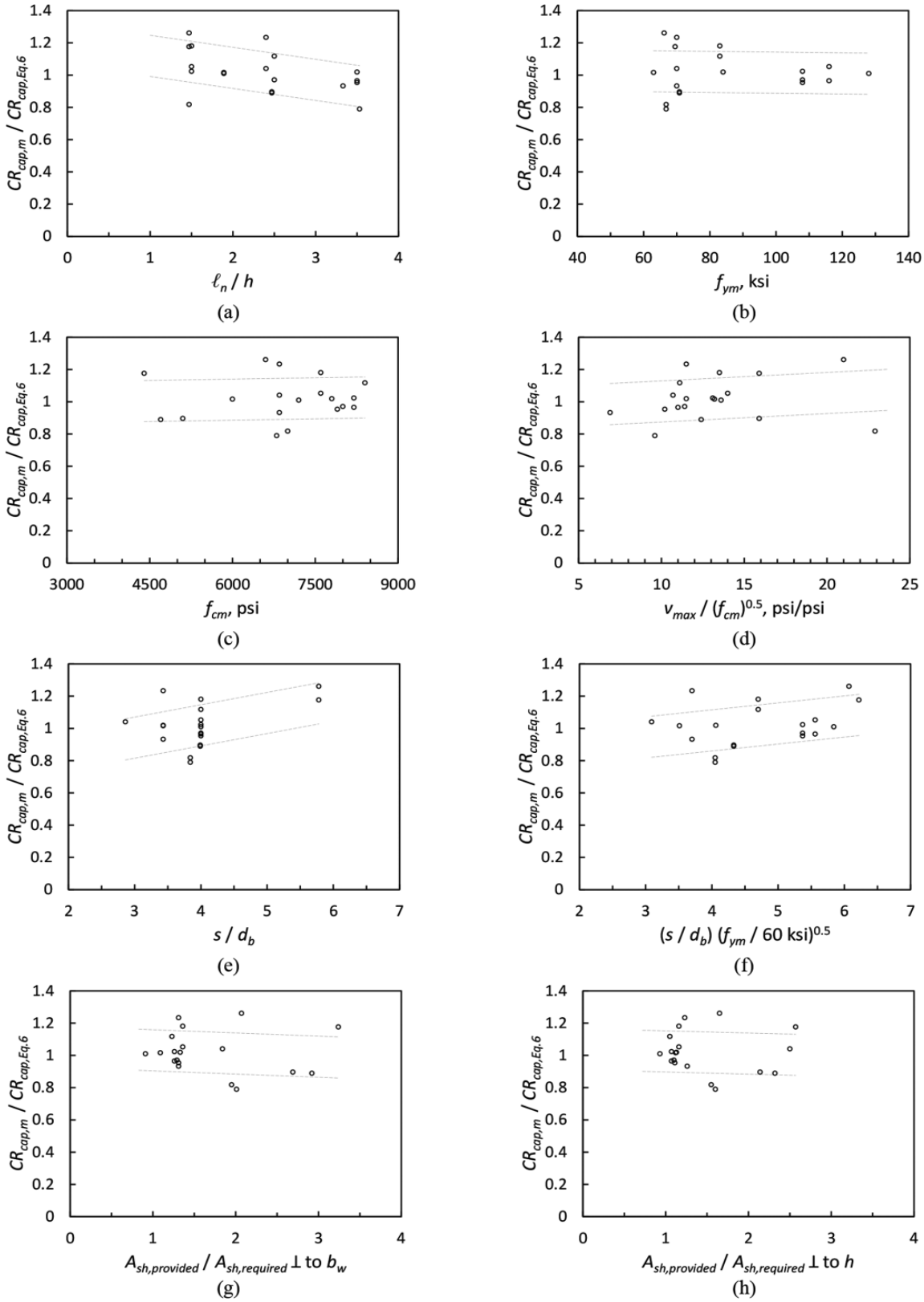

Fig. 4—Measured chord rotation capacity divided by chord rotation capacity calculated with Eq. (6) versus design variables. (Note: 1 ksi = 1000 psi = 6.895 MPa.)

Equation (5) relates $CR_{cap,\text{Eq.(5)}}$ with ℓ_n/h and $\overline{s/d_b}$ for diagonally reinforced coupling beams like those in the analysis database, which included coupling beams with approximately $1 \le \ell_n/h < 4$, $3 \le \overline{s/d_b} \le 6$, $60 \le f_{ym} \le 130$ ksi [$420 \le f_{ym} \le 900$ MPa], and transverse reinforcement satisfying the minimum area required in ACI 318-19 Section 18.10.7.4.[5] Equation (5) was simplified to Eq. (6), an approximation that is appropriate because the analysis database contains only 27 specimens and the design variables are not independently distributed within the database.

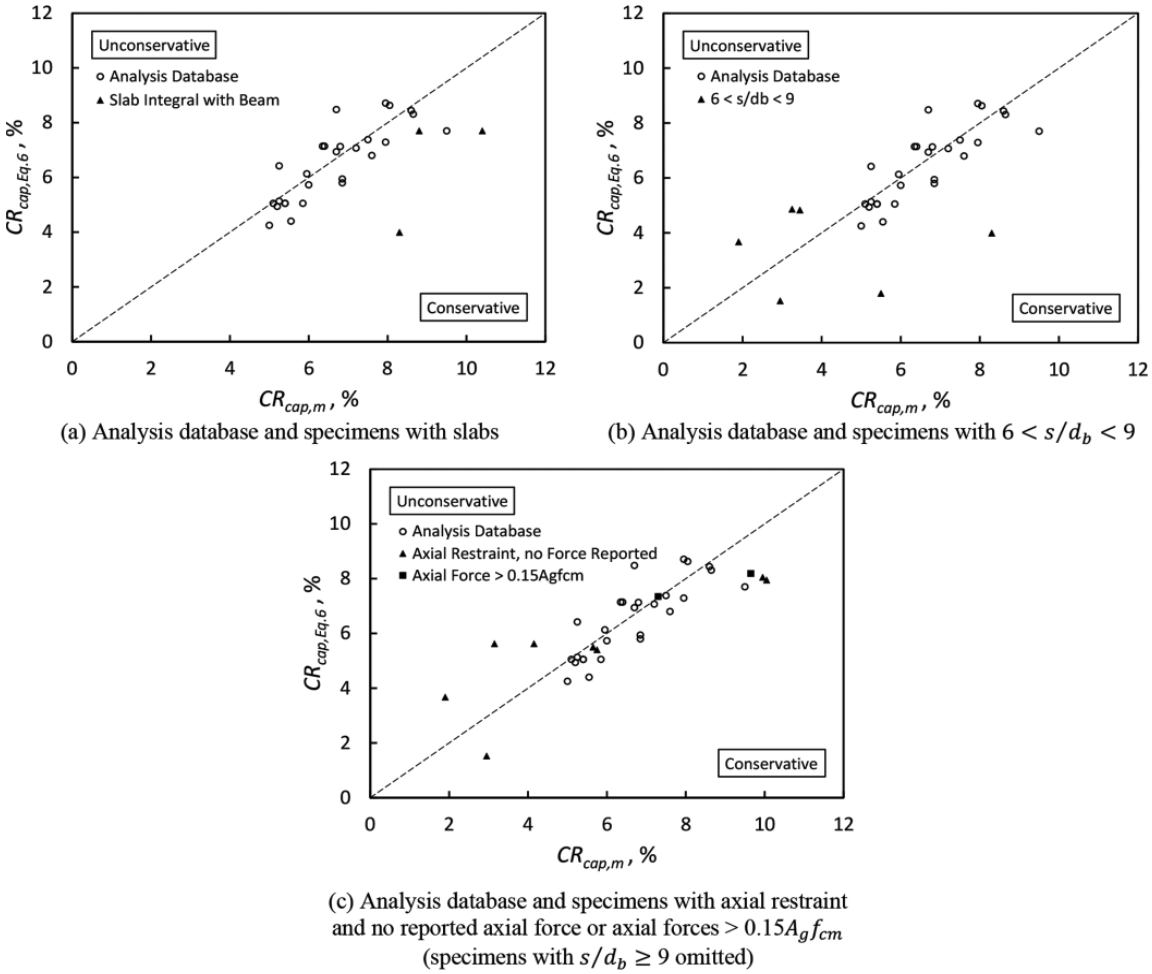

(a) Analysis database and specimens with slabs

(b) Analysis database and specimens with $6 < s/d_b < 9$

(c) Analysis database and specimens with axial restraint and no reported axial force or axial forces > $0.15A_g f_{cm}$ (specimens with $s/d_b \geq 9$ omitted)

Fig. 5—Chord rotation capacity calculated with Eq. (6) versus measured chord rotation capacity for analysis database and selected specimens excluded from analysis database.

$$CR_{cap,\text{Eq.(6)}} = (9 + \ell_n/h - \overline{s/d_b})/100 \quad (6)$$

Further simplification is possible (Eq. (7)) by setting $\overline{s/d_b} = 6$ and therefore neglecting the beneficial effects of having $\overline{s/d_b} < 6$.

$$CR_{cap,\text{Eq.(7)}} = (3 + \ell_n/h)/100 \quad (7)$$

Figure 4 shows $CR_{cap,m}$ divided by $CR_{cap,\text{Eq.(6)}}$ for the specimens in Table 2, plotted versus the same variables considered in Fig. 3. The dotted lines in Fig. 4 represent a linear best-fit line offset by ±σ. The mean and *CV* of $CR_{cap,m}/CR_{cap,\text{Eq.(6)}}$ are 1.03 and 0.11, indicating that Eq. (6) provides a reasonably close estimate of chord rotation capacity. For comparison, the mean and *CV* of the ratio of measured to calculated CR_{cap} are 1.00 and 0.10 for Eq. (5) and 1.26 and 0.16 for Eq. (7). This shows that the loss of either accuracy or precision was negligible when simplifying Eq. (5) to obtain Eq. (6). Equation (7) is less accurate and precise, but also simpler. If a version of these equations were used as a basis for design or evaluation of structures, they should be modified to produce an appropriate level of conservatism.

Effects of variables omitted from analysis database

Some of the specimens omitted from the analysis database represent design conditions that will be found in practice, and it is important to examine how the chord rotation capacities of those specimens compare against the values calculated with Eq. (6). In particular, the effects of slabs built integrally with a coupling beam, hoops with $s/d_b > 6$, and axial restraint are worth assessing even though the available data are limited.

Figure 5 shows $CR_{cap,\text{Eq.(6)}}$ plotted versus measured $CR_{cap,m}$. Specimens in the analysis database are represented with open circles, and relevant specimens from the full database[18] that were omitted from the analysis database are represented with solid triangles and squares. Specimens omitted from the analysis database for reasons unrelated to slabs, hoop spacing, or axial restraint are not included in Fig. 5.

Figure 5(a) shows that the three specimens in the full database[18] that had slabs built integrally with the coupling beam (obtained from Naish et al.[2]) exhibited $CR_{cap,m}$ that were similar to or larger than $CR_{cap,\text{Eq.(6)}}$. This is consistent with the discussion of slab effects in Naish et al.,[2] which noted no detrimental effects of slabs on chord rotation capacity.

Figure 5(b) has solid triangles representing the six specimens from the full database[18] that had $6 < s/d_b < 9$ (obtained

from References 1, 2, and 22 to 24). Two of the six specimens also had axial restraint with no reported axial forces; another had a post-tensioned slab built integrally with the beam. Figure 5(b) shows that $CR_{cap,\text{Eq.(6)}}$ is conservative for half of the specimens with $6 < s/d_b < 9$, but the scatter is also larger for these specimens than specimens within the analysis database. Four of the six specimens with $6 < s/d_b < 9$ also had $CR_{cap,m} < 5\%$, which is less than any of the specimens in the analysis database. The two beams with axial restraint, $6 < s/d_b < 9$, and without slabs had $CR_{cap,m} < 3\%$. Hoop spacings wider than permitted in ACI 318-19[5] therefore appear to have a detrimental effect on chord rotation capacity. This is unsurprising because the deformation capacity of diagonally reinforced coupling beams is often limited by fracture of diagonal bars after buckling in prior loading cycles.

Figure 5(c) has solid triangles representing eight specimens from the full database[18] that had axial restraint, but where the induced axial forces were not reported (obtained from References 22 and 25 to 27), and two solid squares representing the specimens from the full database with peak axial forces larger than $0.15A_gf_{cm}$ (obtained from Poudel et al.[14] and Gonzalez[28]). Figure 5(c) shows that four axially restrained specimens had $CR_{cap,m} < 5\%$, but two of these also had $6 < s/d_b < 9$, so the effects of axial restraint are difficult to isolate (the two specimens with axial restraint and $6 < s/d_b < 9$ had $CR_{cap,m} < 3\%$). The six other axially restrained specimens in Fig. 5(c) had $CR_{cap,m}$ values that were similar to or slightly larger than $CR_{cap,\text{Eq.(6)}}$. Without more data from tests with axial restraint and reported axial forces, it is difficult to draw conclusions about effects of axial restraint on $CR_{cap,m}$ in an aggregated way. Based on a targeted study with four specimens, Poudel et al.[14] observed an approximately 10% reduction of $CR_{cap,m}$ when axial restraint induced axial forces of approximately $0.2A_gf_{cm}$, and negligible effects on $CR_{cap,m}$ when induced axial forces were approximately $0.1A_gf_{cm}$.

COUPLING BEAM STRENGTH

Equation (1), from ACI 318-19 Section 18.10.7.4,[5] gives estimates of coupling beam strength that can be substantially conservative.[10-14] The beam shear corresponding to beam-end moments based on calculated flexural strength is a more accurate estimate of beam strength and allows the engineer to account for effects on strength of developed non-diagonal longitudinal reinforcement, a slab built integrally with the coupling beam, and axial forces.

These prior findings are supported by the results in Table 5, which shows V_m for the 27 specimens in the analysis database and ratios of measured to calculated beam strength based on three calculation methods. Method 1 is the nominal shear strength from Eq. (1), Method 2 is the shear force corresponding to development of M_n at both beam ends, and Method 3 is the shear force corresponding to development of M_{pr} at both beam ends. No strength reduction factors were used to produce Table 5. To calculate $V_{n,\text{Eq.(1)}}$ and M_n, measured material properties (f_{cm} and f_{ym}) were used, which are analogous to the expected material properties recommended in ASCE/SEI 41-17.[6] To calculate M_n, beams were considered doubly reinforced, and the longitudinal component of the diagonal bar areas was used. Concrete compression zone stresses were represented with an equivalent rectangular stress block, and reinforcing bars were assumed to be elastoplastic. The presence of non-diagonal longitudinal reinforcement was neglected in specimens where this reinforcement was cut off near the face of the wall (a detail recommended in Section R18.10.7 of ACI 318-19[5]). Axial forces were considered. The same assumptions were used to calculate M_{pr}, except that $1.1f_{ym}$ was used in place of f_{ym}. If f_{ym} is assumed to be $1.1f_y$, then $1.1f_{ym}$ is similar to the $1.25f_y$ recommended in ACI 318-19[5] for calculating probable flexural strength ($1.1f_{ym} = 1.21f_y \approx 1.25f_y$).

Table 5 shows that Method 1 systematically underestimates beam strength, with a mean measured-to-calculated strength ratio of 1.59 and values as high as 2.46. This is likely too conservative when used to model a coupled wall system, where neglecting beam overstrength can produce unintended and negative effects on wall and foundation behavior.[15,16] Method 2 provides conservative but considerably more accurate and precise estimates of beam strength, with a mean measured-to-calculated ratio of 1.20 and a range of 1.01 to 1.57. Method 3 produces a mean measured-to-calculated ratio of 1.12 and a range of 0.94 to 1.48, indicating it also gives an accurate and generally conservative estimate of expected beam strength. To produce a backbone curve (Fig. 1) with more accurate expected strengths, Methods 2 and 3 are recommended for calculating Q_y and Q_C, respectively.

COUPLING BEAM ENVELOPE RECOMMENDATIONS

Table 6 lists recommendations for a revised force-deformation envelope with parameters corresponding to Fig. 1. Equation (6) is recommended for calculating e, which is the total chord rotation at E. Consistent with ASCE/SEI 41-17[6] recommendations, the total chord rotation at peak strength, d, is taken as 0.02 rad less than e. It is recommended that the coupling beam shear Q_y at B be calculated from M_n at each end of the coupling beam based on expected material properties and that the strength Q_C be calculated from M_{pr} based on expected concrete compressive strength and $1.1f_{y,e}$. No change is recommended to the post-peak residual strength, which is still defined in Table 6 with $c = 0.8$, producing a post-peak strength of $0.8Q_y$. Lastly, Eq. (3) is recommended for calculating I_{eff}/I_g. The recommended envelope is intended to provide an estimate of mean response and has no built-in conservatism. Some modification may be appropriate to produce an acceptable level of conservatism.

Table 6 produces the envelopes plotted in Fig. 6, which includes the measured force-chord rotation data of six specimens from the database. In general, the proposed envelope provides better approximations of beam stiffness than the ASCE/SEI 41-17[6] envelope. The proposed envelope also gives a more realistic estimate of chord rotation capacity, particularly for slender coupling beams ($\ell_n/h > 3$), which consistently exhibit more deformation capacity than the ASCE/SEI 41-17[6] envelope suggests. For the specimens in Fig. 6, both envelopes provide similar estimates of beam strength. It is expected that the recommended strength

Table 5—Coupling beam measured and calculated strengths

Specimen number	Reference	Specimen ID	Measured	Ratio of measured to calculated strength		
			V_m, kip	Method 1* $V_m/V_{n,\text{Eq.(1)}}$	Method 2* $V_m/(2M_n/\ell_n)$	Method 3† $V_m/(2M_{pr}/\ell_n)$
1	Naish et al.[2]	CB24D	157	1.15	1.08	1.00
2		CB24F	161	1.18	1.14	1.05
3		CB33F	117	1.09	1.06	0.98
4	Lim et al.[20]	CB30-DA‡	153	1.46	1.03	0.95
5		CB30-DB‡	160	1.53	1.06	0.99
6	Lim et al.[21]	CB10-1‡	320	1.64	1.05	0.98
7		CB20-1‡	238	1.59	1.01	0.94
8	Cheng et al.[10]	D1.5_H§	352	2.11	1.51	1.40
9		D1.5_H2§	390	2.30	1.49	1.39
10		D1.5_L§	215	2.46	1.57	1.48
11		D2.5_H§	238	1.29	1.03	0.95
12		D2.5_L§	176	1.98	1.17	1.13
13		D3.5_L§	165	1.99	1.44	1.34
14	Ameen et al.[17]	CB1	183	1.31	1.07	0.99
15		CB2‖	200	1.43	1.19	1.11
16		CB2AD‡,§,‖	231	1.66	1.20	1.18
17		CB2D‡,‖	199	1.43	1.07	1.03
18		CB3D‡,‖	272	1.30	1.15	1.10
19	Weber-Kamin et al.[11]	D80-1.5	247	1.46	1.19	1.10
20		D80-2.5	219	1.36	1.16	1.07
21		D80-3.5	219	1.39	1.23	1.14
22		D100-1.5	255	1.39	1.14	1.05
23		D100-2.5	217	1.33	1.15	1.06
24		D100-3.5	194	1.27	1.14	1.09
25		D120-1.5‖	263	1.67	1.34	1.24
26		D120-2.5‡,‖	285	1.89	1.36	1.28
27		D120-3.5‖	214	1.47	1.31	1.25
			Minimum	1.09	1.01	0.94
			Maximum	2.46	1.57	1.48
			Mean	1.59	1.20	1.12
			CV	0.23	0.13	0.13

*Based on f_{cm} and f_{ym}.

†M_{pr} based on f_{cm} and $1.1f_{ym}$.

‡Specimen with non-diagonal longitudinal reinforcement developed into supports.

§Specimen with axial restraint and peak axial force < $0.15A_gf_{cm}$.

‖Specimen with bars exhibiting a so-called "roundhouse" stress-strain curve with no yield plateau.

Note: 1 kip = 4.45 kN.

calculations will be advantageous when there is a slab, axial force, or developed non-diagonal reinforcement, given that the strength calculations do not exclusively depend on the area of the diagonal bars.

Limitations of proposed envelope

The recommendations in Table 6 are intended for diagonally reinforced concrete coupling beams compliant with ACI 318-19.[5] The approach taken in this study was to propose an envelope that represents the expected response, and thus there is little inherent conservatism incorporated in the factors in Table 6. It would likely be appropriate to incorporate some conservatism in estimates of chord rotation capacity. Effects of axial restraint are also not considered in the proposal.

Table 6—Force-deformation envelopes for coupling beams compliant with ACI 318-19[5]

Parameters*		Envelope from ASCE/SEI 41-17[6]	Recommended envelope
Deformation capacity	d	0.03	$(7 + \ell_n/h - \overline{s/d_b})/100$†
	e	0.05	$(9 + \ell_n/h - \overline{s/d_b})/100$†
Strength	Q_y	$V_{n,\text{Eq.(1)}}$‡	$(M_n^+ + M_n^-)/\ell_n$§
	Q_C	V_{pr}‖	$(M_{pr}^+ + M_{pr}^-)/\ell_n$#
	c	0.8	0.8
Stiffness	I_{eff}/I_g	0.3**	0.07 (ℓ_n/h) (60 ksi/f_y)††

*Refer to Notation.

†$\overline{s/d_b}$ may be taken as 6 for coupling beams compliant with ACI 318-19.

‡Equation (1) using $f_{y,e}$.

§M_n based on expected material properties.

‖Equation (1) using a bar stress of $1.25f_{y,e}$.

#M_{pr} based on expected concrete compressive strength and $1.1f_{y,e}$.

**Based on Table 10-5 of ASCE/SEI 41-17.[6]

††From Reference 8, modified as recommended in Reference 17.

Note: 1 ksi = 6.89 MPa.

SUMMARY AND CONCLUSIONS

A database of results from 27 tests of diagonally reinforced concrete coupling beams was analyzed to develop improved force-deformation envelopes for modeling and analysis of coupling beams. The database (Table 2), which was selected from a larger set of 60 test results,[18] comprises specimens that generally satisfy ACI 318-19[5] requirements, except specimens with high-strength reinforcement and shear stresses (based on measured forces) greater than $10\sqrt{f_{cm}}$ psi ($0.83\sqrt{f_{cm}}$ MPa) were also included. The following conclusions were drawn:

1. Within the database, coupling beam chord rotation capacity was correlated with ℓ_n/h and $\overline{s/d_b} = (s/d_b)(\sqrt{f_{ym}/60\text{ ksi}})$ $[(s/d_b)(\sqrt{f_{ym}/420\text{ MPa}})]$.

2. After accounting for correlations with ℓ_n/h and $\overline{s/d_b}$, coupling beam chord rotation capacity was not strongly correlated with $v_{max}/\sqrt{f_{cm}}$, f_{ym}, f_{cm}, or the quantity of transverse reinforcement, as long as the quantity of transverse reinforcement exceeded that required in ACI 318-19.[5]

3. The chord rotation capacity of coupling beams such as those in the analysis database can be estimated with Eq. (6) (reproduced as Eq. (8)). The equation gives mean and CV values of 1.03 and 0.11 for measured-to-calculated ratios. The equation is based on a database of diagonally reinforced concrete coupling beams with approximately $1 \le \ell_n/h \le 4$, $3 \le \overline{s/d_b} \le 6$, $60 \le f_{ym} \le 130$ ksi (420 and 900 MPa), and $4 \le 2A_{vd}f_{ym}\sin\alpha/(b_w h\sqrt{f_{cm}\text{ (psi)}}) \le 15$ $(0.33 \le 2A_{vd}f_{ym}\sin\alpha/(b_w h\sqrt{f_{cm}\text{ (MPa)}}) \le 1.25)$.

$$CR_{cap,\text{Eq.(6)}} = (9 + \ell_n/h - \overline{s/d_b})/100 \quad (8)$$

4. The limited data support prior observations[9] that slabs built integrally with a coupling beam do not reduce $CR_{cap,m}$.

5. Beams with $6 < s/d_b < 9$ tend to exhibit reduced $CR_{cap,m}$. Four of the six specimens with $6 < s/d_b < 9$ had $CR_{cap,m} < 5\%$, which is less than any of the coupling beams in the analysis database.

6. It is difficult to draw conclusions about the effects of axial restraint on $CR_{cap,m}$ in an aggregated way without more data from tests with axial restraint and reported axial forces. Prior work[14] found a negative effect on $CR_{cap,m}$ for axial forces of approximately $0.2A_gf_{cm}$.

7. Analyses support prior findings that coupling beam strength is more accurately estimated using the nominal flexural strength at beam ends than the nominal shear strength (Eq. (1)). Strengths based on $(M_n^+ + M_n^-)/\ell_n$ and $(M_{pr}^+ + M_{pr}^-)/\ell_n$ had mean ratios of measured-to-calculated strengths of 1.2 and 1.1, respectively, both with a CV of 0.13. Strengths based on Eq. (1) had a mean measured-to-calculated strength ratio of 1.6 with a CV of 0.23.

AUTHOR BIOS

Andrés Lepage, *FACI, is a Professor at The University of Kansas, Lawrence, KS. He is a member of ACI Committees 318, Structural Concrete Building Code; 374, Performance-Based Seismic Design of Concrete Buildings; and 375, Performance-Based Design of Concrete Buildings for Wind Loads; and Joint ACI-ASCE Committee 335, Composite and Hybrid Structures.*

ACI member **Rémy D. Lequesne** *is the Stanley T. and Phyllis W. Rolfe Chair's Council Associate Professor at The University of Kansas. He is Chair of Joint ACI-ASCE Committee 408, Bond and Development of Steel Reinforcement, and a member of ACI Committee 133, Disaster Reconnaissance; ACI Subcommittee 318-J, Joints and Connections; and Joint ACI-ASCE Committee 352, Joints and Connections in Monolithic Concrete Structures.*

Alexander S. Weber-Kamin *is a Research and Design Engineer in the Structural Engineering Department and the Caltrans Seismic Response Modification Device Test Facility at the University of California, San Diego, La Jolla, CA. They received their BS from The University of Oklahoma, Norman, OK, and their PhD from The University of Kansas.*

Shahedreen Ameen *is a Project Consultant at Simpson Gumpertz & Heger Inc., New York, NY. She received her BS from Bangladesh University of Engineering and Technology, Dhaka, Bangladesh, and her PhD from The University of Kansas.*

ACI member **Min-Yuan Cheng** *is a Professor in the Department of Civil and Construction Engineering at National Taiwan University of Science and Technology, Taipei, Taiwan. He is a member of ACI Subcommittee 318-J, Joints and Connections, and Joint ACI-ASCE Committee 352, Joints and Connections in Monolithic Concrete Structures.*

ACKNOWLEDGMENTS

Financial support from the following sources is gratefully acknowledged: The University of Kansas Department of Civil, Environmental & Architectural Engineering; the Charles Pankow Foundation; the ACI Foundation's Concrete Research Council; and the Concrete Reinforcing Steel Institute.

NOTATION

A_g = gross area of concrete section, in.^{2} (mm^2)
$A_{sh,provided}$ = cross-sectional area of transverse reinforcement provided within s, in.^{2} (mm^2)
$A_{sh,required}$ = cross-sectional area of transverse reinforcement within s required in ACI 318-19, Section 18.10.7.4,[5] $=0.09sb_cf_{cm}/f_{ytm}$, in.^{2} (mm^2)
A_{vd} = total area of reinforcement in each group of diagonal bars, in.^{2} (mm^2)
b_c = cross-sectional dimension measured to outside edges of hoops, in. (mm)
b_w = beam width, in. (mm)
$CR_{cap,\text{Eq.(X)}}$ = chord rotation capacity calculated with Eq. (X), rad
$CR_{cap,m}$ = average of maximum chord rotations in each loading direction where envelope of shear versus chord rotation curve (formed by connecting maximum chord rotation of first

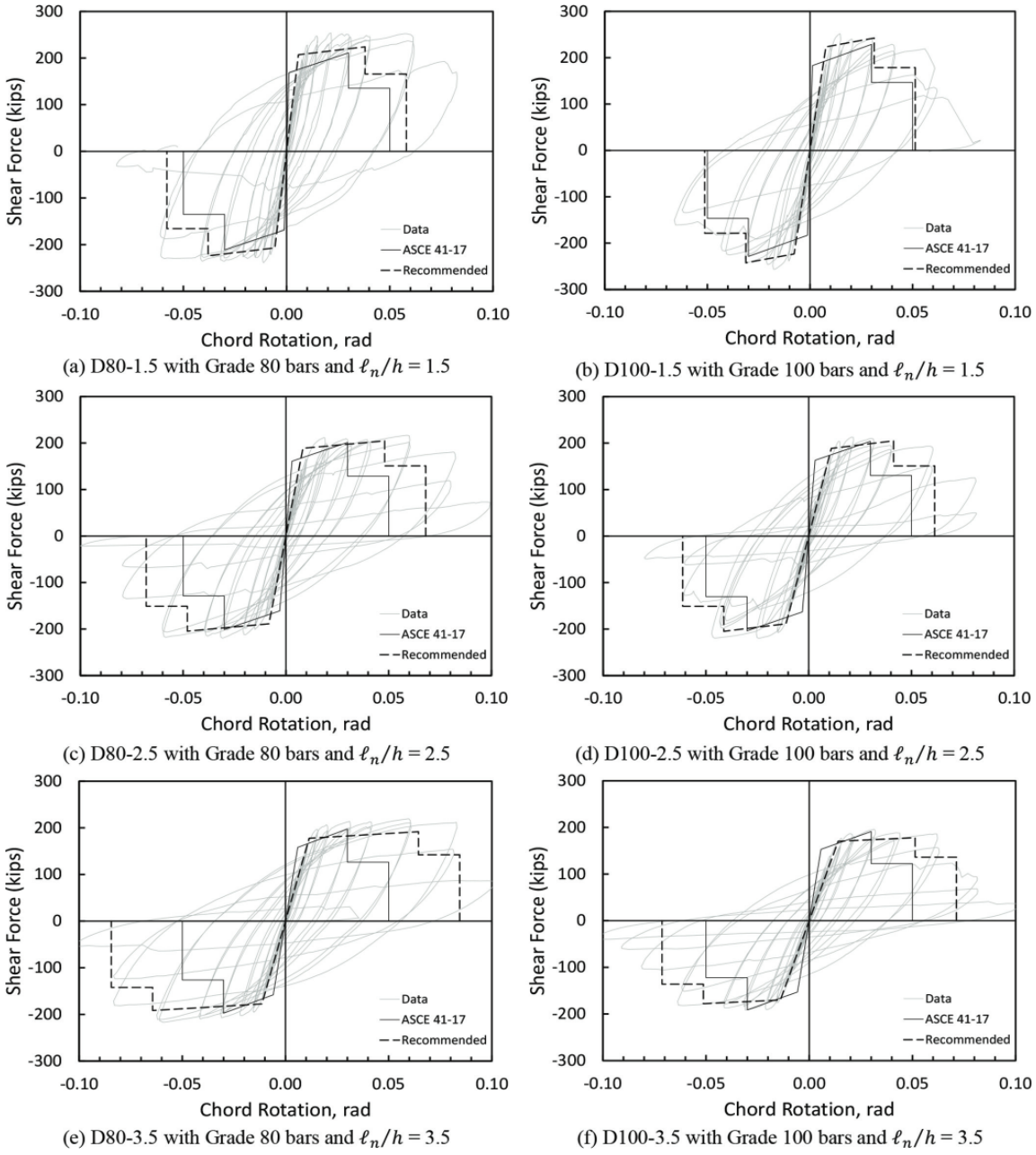

Fig. 6—Results from tests of diagonally reinforced concrete coupling beams compliant with ACI 318-19[5] from Weber-Kamin et al.[11] and envelopes from Table 6. (Note: 1 kip = 4.45 kN.)

cycle of each loading step) intersects 80% of maximum applied shear, rad

CV = coefficient of variation, ratio of standard deviation to mean
c = parameter used to quantify residual strength (Fig. 1)
c_0, c_1 = intercept and slope of best-fit line defined by Eq. (4)
d = parameter used to quantify total deformation to capping point C (Fig. 1)
d_b = diameter of diagonal bar, in. (mm)
d_{bp} = diameter of parallel bar, in. (mm)
d_{bt} = diameter of transverse bar, in. (mm)
e = parameter used to quantify total deformation to point E (Fig. 1)
f_c' = specified concrete compressive strength, psi (MPa)
f_{cm} = measured concrete compressive strength, psi (MPa)
f_y = specified yield stress, ksi (MPa)
$f_{y,e}$ = expected yield stress; refer to ASCE/SEI 41-17,[6] ksi (MPa)
f_{ym}, f_{ytm} = measured yield stress of diagonal and transverse reinforcement, ksi (MPa)
h = overall depth of beam, in. (mm)
I_{eff} = effective moment of inertia about centroidal axis, in.^{4} (mm^4)
I_g = moment of inertia of gross concrete section about centroidal axis, neglecting reinforcement, in.^{4} (mm^4)
ℓ_n = beam clear span length, in. (mm)
M_n = calculated nominal flexural strength corresponding to stress of $1.0f_y$, $1.0f_{ym}$, or $1.0f_{y,e}$ in diagonal reinforcement, kip·in. (kN·m) (+/− identify loading direction)
M_{pr} = calculated probable flexural strength corresponding to stress of $1.25f_y$, $1.1f_{ym}$, or $1.1f_{y,e}$ in diagonal reinforcement, kip·in. (kN·m) (+/− identify loading direction)
Q = force (Fig. 1), kip (kN)
Q_C = force at capping point C (Fig. 1), kip (kN)
Q_y = force at point B (Fig. 1), kip (kN)
r^2 = coefficient of determination
s = transverse reinforcement spacing, in. (mm)
s/d_b = normalized hoop spacing-to-bar diameter ratio = $(s/d_b)(\sqrt{f_{ym}/60\text{ ksi}})[(s/d_b)(\sqrt{f_{ym}/420\text{ MPa}})]$
V_m = maximum measured shear force, kip (kN)
$V_{n,\text{Eq.(1)}}$ = nominal shear strength per Eq. (1), kip (kN)
V_{pr} = probable shear strength per Eq. (1) using bar stress of $1.25f_y$, $1.1f_{ym}$, or $1.1f_{ye}$, kip (kN)

v_{max} = maximum shear stress $V_m/(b_w h)$, psi (MPa)
X_i = variable in Eq. (4) to evaluate correlation with $CR_{cap,m}$
α = inclination of diagonal bars relative to beam longitudinal axis, degrees
σ = standard deviation

REFERENCES

1. Paulay, T., and Binney, J. R., "Diagonally Reinforced Coupling Beams of Shear Walls," *Shear in Reinforced Concrete*, SP-42, American Concrete Institute, Farmington Hills, MI, 1974, pp. 579-598.

2. Naish, D.; Fry, A.; Klemencic, R.; and Wallace, J., "Reinforced Concrete Coupling Beams—Part 1: Testing," *ACI Structural Journal*, V. 110, No. 6, Nov.-Dec. 2013, pp. 1057-1066.

3. ACI Committee 318, "Building Code Requirements for Structural Concrete (ACI 318-99) and Commentary (ACI 318R-99)," American Concrete Institute, Farmington Hills, MI, 1999, 369 pp.

4. ASCE/SEI 7-16, "Minimum Design Loads and Associated Criteria for Buildings and Other Structures," American Society of Civil Engineers, Reston, VA, 2017, 822 pp.

5. ACI Committee 318, "Building Code Requirements for Structural Concrete (ACI 318-19) and Commentary (ACI 318R-19) (Reapproved 2022)," American Concrete Institute, Farmington Hills, MI, 2019, 624 pp.

6. ASCE/SEI 41-17, "Seismic Evaluation and Retrofit of Existing Buildings," American Society of Civil Engineers, Reston, VA, 2017, 576 pp.

7. ACI Committee 369, "Seismic Evaluation and Retrofit of Existing Concrete Buildings—Code and Commentary (ACI CODE-369.1-22)," American Concrete Institute, Farmington Hills, MI, 2022, 125 pp.

8. TBI, "Guidelines for Performance-Based Seismic Design of Tall Buildings (Tall Buildings Initiative)," Report No. 2017/06, Pacific Earthquake Engineering Research Center, University of California, Berkeley, Berkeley, CA, 2017, 145 pp.

9. Naish, D.; Fry, A.; Klemencic, R.; and Wallace, J., "Reinforced Concrete Coupling Beams—Part II: Modeling," *ACI Structural Journal*, V. 110, No. 6, Nov.-Dec. 2013, pp. 1067-1076.

10. Cheng, M.-Y.; Gitomarsono, J.; and Zeng, H.-Y., "Cyclic Test of Diagonally Reinforced Concrete Coupling Beam with Different Shear Demand," *ACI Structural Journal*, V. 116, No. 6, Nov. 2019, pp. 241-250. doi: 10.14359/51718010

11. Weber-Kamin, A. S.; Lequesne, R. D.; and Lepage, A., "Reinforced Concrete Coupling Beams with High-Strength Steel Bars," SM Report No. 143, The University of Kansas Center for Research, Inc., Lawrence, KS, 2020, 598 pp.

12. Lequesne, R. D., "Behavior and Design of High-Performance Fiber-Reinforced Concrete Coupling Beams and Coupled-Wall Systems," PhD dissertation, University of Michigan, Ann Arbor, MI, 2011, 277 pp.

13. Ameen, S.; Lequesne, R. D.; and Lepage, A., "Diagonally-Reinforced Concrete Coupling Beams with High-Strength Steel Bars," SM Report No. 138, The University of Kansas Center for Research, Inc., Lawrence, KS, 2020, 346 pp.

14. Poudel, A.; Ameen, S.; Lequesne, R. D.; and Lepage, A., "Diagonally Reinforced Concrete Coupling Beams: Effects of Axial Restraint," *ACI Structural Journal*, V. 118, No. 6, Nov. 2021, pp. 293-303.

15. Malcolm, R. C.; Bull, D. K.; Henry, R. S.; and Ingham, J. M., "The Effects of Axial Restraint in Reinforced Concrete Coupling Beams," *Proceedings of the New Zealand Concrete Industry Conference*, Taupō, New Zealand, 2014, pp. 150-159.

16. Cheng, M.-Y.; Fikri, R.; and Chen, C.-C., "Experimental Study of Reinforced Concrete and Hybrid Coupled Shear Wall Systems," *Engineering Structures*, V. 82, 2015, pp. 214-225. doi: 10.1016/j.engstruct.2014.10.039

17. Ameen, S.; Lequesne, R. D.; and Lepage, A., "Diagonally Reinforced Concrete Coupling Beams with Grade 120 (830) High-Strength Steel Bars," *ACI Structural Journal*, V. 117, No. 6, Nov. 2020, pp. 199-210.

18. Weber-Kamin, A. S.; Ameen, S.; Lequesne, R. D.; and Lepage, A., "PRJ-3053 - Database of Diagonally-Reinforced Concrete Coupling Beams," Designsafe-ci.org, 2021. doi: 10.17603/ds2-46wc-n185

19. Lepage, A.; Lequesne, R. D.; Weber-Kamin, A. S.; and Ameen, S., "Chord Rotation Capacity of Diagonally-Reinforced Concrete Coupling Beams," *12th National Conference on Earthquake Engineering*, Salt Lake City, UT, 2022, Paper No. 10806.

20. Lim, E.; Hwang, S.-J.; Cheng, C.-H.; and Lin, P.-Y., "Cyclic Tests of Reinforced Concrete Coupling Beam with Intermediate Span-Depth Ratio," *ACI Structural Journal*, V. 113, No. 3, May-June 2016, pp. 515-524. doi: 10.14359/51688473

21. Lim, E.; Hwang, S.-J.; Wang, T.-W.; and Chang, Y.-H., "An Investigation on the Seismic Behavior of Deep Reinforced Concrete Coupling Beams," *ACI Structural Journal*, V. 113, No. 2, Mar.-Apr. 2016, pp. 217-226.

22. Howard, B., "Seismic Response of Diagonally Reinforced Coupling Beams with Varied Hoop Spacings," MS thesis, McGill University, Montreal, QC, Canada, 2017, 99 pp.

23. Kwan, A. K. H., and Zhao, Z.-Z., "Cyclic Behaviour of Deep Reinforced Concrete Coupling Beams," *Proceedings of the Institution of Civil Engineers - Structures and Buildings*, V. 152, No. 3, 2002, pp. 283-293. doi: 10.1680/stbu.2002.152.3.283

24. Shimazaki, K., "De-Bonded Diagonally Reinforced Beam for Good Repairability," *Proceedings of the 13th World Conference on Earthquake Engineering*, Vancouver, BC, Canada, 2004, Paper No. 3173.

25. Han, S. W.; Kang, J.-W.; Jee, H.-W.; Shin, M.; and Lee, K., "Cyclic Behavior of HPFRCC Coupling Beams with Bundled Diagonal Bars," *International Journal of Concrete Structures and Materials*, V. 12, No. 1, 2018, Article No. 42. doi: 10.1186/s40069-018-0271-6

26. Han, S. W.; Lee, C. S.; Shin, M.; and Lee, K., "Cyclic Performance of Precast Coupling Beams with Bundled Diagonal Reinforcement," *Engineering Structures*, V. 93, 2015, pp. 142-151. doi: 10.1016/j.engstruct.2015.03.034

27. Park, W.-S.; Kang, T. H.-K.; Kim, S.; and Yun, H.-D., "Seismic Performance of Moderately Short Concrete Coupling Beams with Various Reinforcements," *ACI Structural Journal*, V. 117, No. 3, May 2020, pp. 141-154.

28. Gonzalez, E., "Seismic Response of Diagonally Reinforced Slender Coupling Beams," MS thesis, The University of British Columbia, Vancouver, BC, Canada, 2001, 164 pp.